Granular Glasses

Dave A. WEITZ
Department of Physics & SEAS
Harvard University
29 Oxford St.
Cambridge, MA 02138 USA

1   Introduction

At first glance, the sand on a beach and the glass in a window are vastly different. Sand sticks to your feet and makes the floor of your house dirty, much to the dismay of your mother or spouse. The glass in your window keeps the sand out of your house when the wind blows, while letting you look out and admire the view of the beach, should you be so lucky as to have such a beautiful view. However, despite these differences, the two materials share a surprising amount in common. Of course, the sand is primarily silica, and this can be made into glass. However, the similarities go much deeper.

A glass is a material that has the same structure as a liquid. What distinguishes it from a liquid is its very slow relaxation time. In a liquid, thermal motion causes the molecules to constantly move, and these fluctuations lead to relaxation of the structure on short time scales. This structural relaxation is directly manifested in the viscosity of the fluid; for a fluid to flow, its structure must relax, and this relaxation is reflected directly in its viscosity. As a liquid approaches its glass transition, this structural relaxation becomes increasingly slow, ultimately taking longer than any experimental time scale. This leads to a dramatic increase in the viscosity of the liquid. Indeed, one definition of a glass is when the viscosity approaches 10^{12} Poise, which corresponds to flow that will take longer than a day [AMO86]. A glass can, in principle, be made to flow by applying a shear stress, although of course, many glasses will fracture or break before this happens. However, if the glass is not too brittle, and its elastic modulus is not too large, shear will lead to structural relaxation and the glass will flow. Alternatively, heating the glass above its glass transition will also lead to flow.

Sand, or any other granular material, is also a highly disordered structure [JNB96b, JNB96a]. However, it does not typically seem to be a fluid, so it is difficult to compare the structure of sand to that of a fluid. Nevertheless, if sand is shaken, it can flow like a fluid. This can be seen if a bucket of dry sand is turned gently on its side so the top of the sand begins to fall. If this is done slowly enough, the sand flows much like a fluid. An even better example of this is observed if air is gently blown up through sand [MD97]. If the flow rate is set exactly right, the level of the sand rises ever so slightly and the sand becomes fluidized, as is immediately seen if you try to run your hand through it; it feels much more like a fluid than a solid, and the grains of sand flow around your hand as you draw it through the grains. In this case, however, it is not thermal motion that is responsible for the fluidization,

but instead it is the forces of the air blowing up through the grains. Thus, granular materials differ significantly from glasses because thermal energy is not sufficient to cause the individual grains to move; structural relaxation, and hence fluidization, can only occur through the addition of some larger form of energy, such as shaking or blowing air through the medium. However, if the grains are fluidized in this fashion, they can then explore their phase space, and they can behave very much like a fluid. Moreover, as this structural relaxation ceases, a granular material looses its ability to structurally relax, and retains the same structure it had, very much like a glass.

The similarity between glasses and granular material has been elegantly described through the concept of 'jamming', and the associated jamming phase diagram [LN98]. The original jamming phase diagram has three control parameters, the value of which each defines an axis on the graph. One axis is the temperature, which provides a measure of how the system explores its phase space. For a glass, this is just the temperature of the system, whereas for a granular material some other mechanism must cause the system to explore its phase space and this effectively becomes the temperature. The second axis is a measure of the density. For a glass, this is a measure of the expansion of the system whereas for a granular material, this is a measure of the volume fraction of the grains. The third axis is the amount of shear stress applied to the system. The temperature is plotted as the inverse of the temperature, so a decrease in the temperature leads to an increase along the axis. Similarly, the volume fraction or density is also plotted as the inverse, again leading to a lower volume fraction resulting in an increase along the axis. When plotted in this fashion, the innermost quadrant becomes the jammed, or solid phase, and increasing along any three of the axes leads to a point where the system is fluidized. Thus there is a surface on the phase diagram that corresponds to the jamming transition for granular materials or the glass transition for glasses.

The jamming picture provides an elegant means to compare glasses and granular materials, and highlights the similarity in their behavior. However, several essential differences remain. Perhaps the most stark difference is the means by which each system is fluidized. A glass depends on temperature for its fluidization, and it falls out of equilibrium, and becomes a glass, as the temperature is lowered. By contrast, thermal energy has no effect on a granular material, as it is an athermal system; however, it too must fluidized, and this must come from the addition of energy in some other form.

There is one system that shares many of the features of both glasses and granular matter. This system is a colloidal dispersion. Colloids are solid particles immersed in a fluid. The particles are small enough that they undergo Brownian motion. Typically the particles are less than a few microns in size. Their Brownian motion ensures that the colloidal particles sample their phase space and are therefore thermalized. However, the size of the particles is larger than that of the molecules in a typical glass, and the granularity of the particles has important implications for their behavior. Thus, colloidal particles fall between traditional molecular glasses and traditional granular materials. They have the behavior of "granular glasses". Their behavior offers insight into both traditional glasses and granular materials. This paper will explore some examples of this.

Colloidal particles are of great interest in themselves, as they can model the behavior of many complex fluid systems. However, even more interesting is the

scale of the particles and the control that is possible over their properties. The particles can be synthesized with exquisite precision, leading to nearly perfectly monodispersity in particle size, with variations of less than a few percent in their radii. Moreover the interparticle interactions can be precisely controlled and easily tuned. Perhaps the most intriguing feature of their study is that their size, being around one micron, is ideal for visualization in an optical microscopy [VBW95]; moreover, the time scale of their motion is sufficiently slow that their dynamics can be followed in real time. A typical time scale is given by the time it takes to move their own diameter; since the particles are in a fluid, their microscopic motion is diffusive, and a typical diffusion time, given by $\tau = a^2/D_0$, ranges from msec to sec. Here, a is the particle radius and $D_0 = k_B T/6\pi\eta a$ is the Stokes-Einstein diffusion coefficient of an isolated particle in solution, where k_B is Boltzmann's constant and η is the viscosity of the fluid. With modern confocal microscopy, it is now possible to follow the motion of individual particles over time in 3D; up to 10,000 particles can be followed simultaneously. Because the particles are all the same shape and are spherical, their diffraction pattern is known; thus the precision with which the location of the particle centers can be located is given by signal-to-noise, rather than the more commonly assumed Rayleigh diffraction limit; thus it is possible to identify the location of each particle to within a few percent of its radius [CG96]. This offers the opportunity to explore their dynamics with unprecedented precision, and provides new insight into the behavior of these 'granular glasses.'

2   Repulsive Colloidal Glasses

In order to ensure that colloidal particles remain suspended, it is essential that they do not stick together upon random collisions that invariably occur. Thus, all stable colloidal colloids possess some form of repulsive interaction between the particles. The simplest of these is through volume exclusion; the particles can not occupy the same volume. This requires a very strong, yet very short-range repulsive interaction between particles. There is no interaction except when two particles touch, and then the interaction is very strongly repulsive. Such colloidal particles then behave as hard spheres [PVM86].

Hard-sphere colloidal particles exhibit a glass transition [PVM87]. However, since there is no repulsive energy between the particles, except when they exactly touch, the enthalpic term of the free energy can be neglected, and the only contribution to the free energy of the system is entropic. Moreover, the temperature of the suspension can only be changed a relatively small amount before its properties are significantly modified. For example, the continuous fluid can either boil of freeze, and in either case, the colloidal suspension would no longer behave as a suspension. In fact, much smaller temperature changes usually suffice to drastically modify the properties of the suspension, and as a result, temperature is typically not a good control parameter for colloidal particles. Instead, the control parameter is the entropy, and this is controlled by varying the particle volume fraction, ϕ. Perfectly uniform, or monodisperse, spherical particles will undergo a crystallization transition at $\phi = 0.494$, and will coexist with a fluid-like order of the particles up to $\phi = 0.55$, whereupon the sample will remain crystalline up to the maximum packing of the face-centered cubic lattice that forms, $\phi = 0.74$ [PVM86]. However, if the sample is rapidly quenched to a higher volume fraction, the structural relaxation

that is essential for it to undergo crystallization is suppressed: The particles become increasingly crowded as ϕ increases, making it increasingly difficult for the particles to move and to undergo structural relaxation. As the particles become increasingly crowded, the structural relaxation time becomes increasingly larger. This behavior has all the hallmarks of a glass transition [PVM87]. This has been rather widely investigated as the behavior is well described using mode-coupling theory, which describes the shape of the relaxation as measured with light scattering, and correctly accounts for the divergence of the structural relaxation time [VMU93].

One of the most direct manifestations of the onset of a glassy state is shown by the mechanical response of the suspension, which can be measured with a rheometer [MW95]. We use a sample of silica spheres suspended in ethylene glycol, where they interacted as hard spheres. The particle radius was $a = 0.21\mu$m, with a polydispersity in radius of about 20%, which prevented crystallization. The sample was held between the walls of a double-walled Couette geometry, enabling sensitive measurement of the mechanical response. The rheometer was controlled-strain, and applied a known strain at a given frequency and measured the resultant stress at the same frequency. Frequency dependent measurements of the real, or elastic, $G'(\omega)$, and the imaginary, or viscous, $G''(\omega)$, moduli are shown respectively in the upper and lower parts of Fig. 1.At the lower ϕ, $G''(\omega)$ is dominant, and both moduli increase with frequency. However, as ϕ increases, $G'(\omega)$ begins to dominate over an extended range of frequencies; moreover, it develops a plateau where it varies only very slowly with frequency, while $G''(\omega)$ exhibits a definite and reproducible minimum. At higher frequencies, both moduli begin to increase, with $G''(\omega)$ rising more sharply, ultimately overtaking $G'(\omega)$. We can describe this behavior using the same theoretical approach that was used to account for the structural relaxation. We use a mode-coupling theory that also includes a contribution of the fluid at high frequencies, where it must begin to dominate the measured response. The results are in excellent agreement with the data, as shown by the solid lines in Fig 1 [MW95]. This is direct evidence that the colloidal suspension behaves like a glass.

The important properties to note in the data in Fig. 1 are the fact the elastic, or storage modulus, $G''(\omega)$, is greater than the viscous, or loss modulus, $G''(\omega)$, over an extended range of frequencies, including those that are most "apparent" to common use. This implies that the material is behaving like a solid, and does exhibit a shear modulus, over these frequencies. At lower frequencies, the material undergoes structural relaxation; this relaxation extends to lower and lower frequencies as the volume fraction of particles increases, and will ultimately become so large that it can not be measured with these techniques: This is the glass transition. These data highlight the fact that the control parameter for colloidal hard spheres is volume fraction rather than temperature, and that an increase in ϕ corresponds to a decrease in T, reflecting the correspondence of ϕ^{-1} to T. Because there is no interparticle interaction energy, the solid-like behavior of the particles must result from purely entropic origins.

To explore the origin of this elasticity, we use confocal microscopy to visualize the particle motion as the glass transition is approached [WCL$^+$00]. This allows us to monitor the motion of the particles, and to observe the nature of the structural relaxation. For these experiments, we use poly-(methylmethacrylate) particles, sterically stabilized by a thin layer of poly-12-hydroxystearic acid [AGH86]. The particles have a radius $a \approx 1.18\mu$m, a polydispersity of $\approx 5\%$, and are dyed with rhodamine
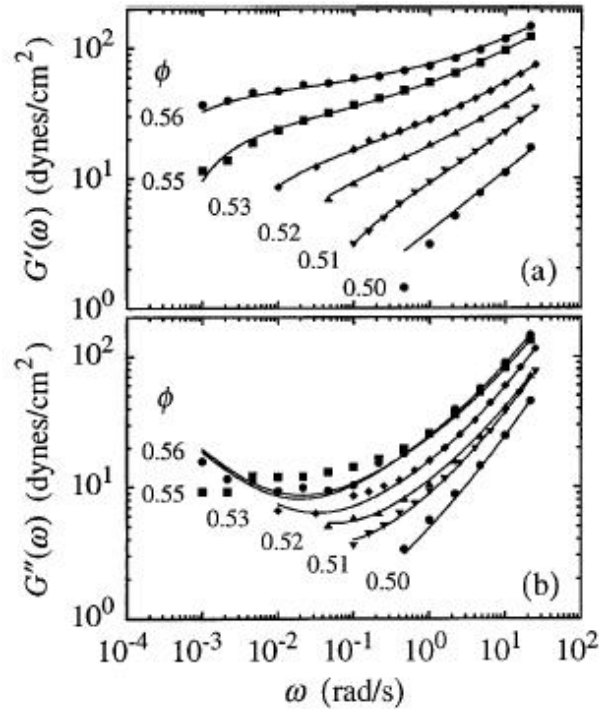
Figure 1: The frequency dependences of the (a) storage and (b) loss moduli for different volume fractions. All the measurements were performed at sufficiently low strains to be in the linear regime. The solid lines represent the fit to the mode-coupling model

and suspended in a cycloheptylbromide/decalin mixture which nearly matches both the density and the index of refraction of the particles. We track particles for the entire duration of the experiment. We determine ϕ for each sample by measuring the volume per particle directly with the microscope.

The motion of the individual particles is very revealing: We plot the trajectories of several particles as they evolve in time in Fig. 2; the grey shading indicates depth in the third dimension. Each particle is trapped in some local volume, with its trajectory moving only a small fraction of its size, until, at some random time, the particle moves a much larger amount, whereupon it is again trapped in a more localized volume. All particles that we investigate share this same characteristic motion. This motion reflects the nature of the structural relaxation. Physically, each particle is trapped in a cage composed of its neighbors, due to the crowding of the particles. Over the course of this cage-trapping time, the mean square displacement of the particle is almost independent of time; this also corresponds directly to the frequencies over which the elastic modulus exhibits the plateau in Fig. 1. Eventually, the cage of neighbors surrounding the particle relaxes sufficiently that it moves, and when it does, it moves a rather larger distance. This results in structural relaxation of the system, and corresponds to the lowest frequencies in Fig. 1, where the elasticity falls. These results provide important insight into the origin of the elasticity: During the time that the particle is trapped in its cage, its most probable position is within this cage; a small shear strain, as is applied to measure the elasticity, distorts the shape of the cage, reducing the number of configurations that the particle can sample by straining the cage. This results in an increase in energy. If the strain is removed

before the cage relaxes, the larger number of configurations are restored, and the energy is reduced. This storage of energy is directly reflected in the elasticity of the sample. It is strictly entropic in origin.
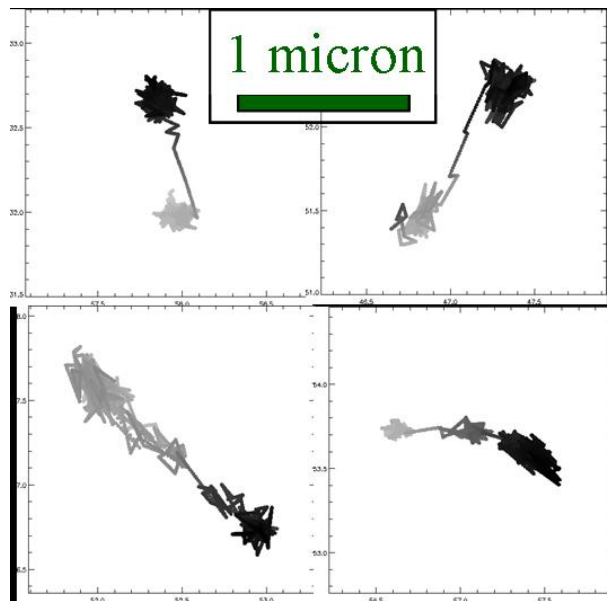

Figure 2: Temporal traces of the position of 4 different particles in a sample with a volume fraction of $\phi = 0.56$, near the glass transition, exhibiting cage trapping and cage escape. Grey shading indicated depth.

The characteristic time of the structural relaxation can be determined from the frequency of the relaxation measured with the rheological measurements, or from the mean square displacement of the particles, which exhibits an upturn at times corresponding to the structural relaxation frequency [WCL+00, WW02]. If we measure the motion of the particles on that time scale, we highlight the motion corresponding to the structural relaxation. When this is done, we observe that the structural relaxation of the particles is not uniformly distributed in space; instead, the motion of the relaxing particles in highly correlated among neighbors. To demonstrate this, we plot the particles in uniform time intervals of 5 minutes, and show those particles that have moved a large amount, and hence have undergone structural relaxation in the previous time interval, as red particles, drawn to scale, while those particles that have remained trapped are plotted as blue particles, and are drawn smaller, enabling the full 3D image to be visualized. Surprisingly, the moving particles are very strongly correlated in space, as show in Fig. 3. When one particle moves, it clearly opens a space behind it, through which a neighboring particle can move. This large scale correlation between the relaxing particles is what drives the longer relaxation times; it is not sufficient to have only a single particle to move, but rather a large number of particles must move collectively to enable structural relaxation. We can define a length scale for these correlated motion by measuring the average size of regions of nearest-neighbor particles that undergo this structural relaxation. The average size increases dramatically as the volume fraction approaches the glass transition, $\phi_g \approx 0.58$, but then decreases to essentially zero above ϕ_g, as show in Fig. 4. The structural relaxation is clearly very heterogenous in both space and

time. Similar behavior occurs in molecular glass formers, where this motion is referred to as dynamic heterogeneities [SRS91, CE95]. However, direct observation of such behavior is not feasible with molecular glass formers, whereas with colloidal particles it is readily seen. Instead, besides colloidal particles, it is seen in computer simulation [DGP99].
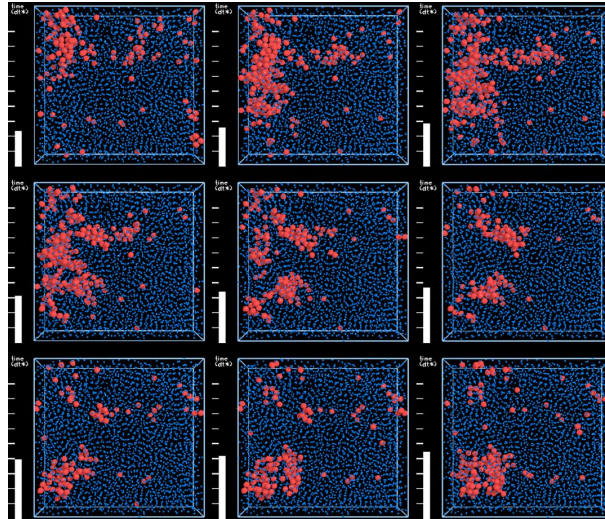

Figure 3: Correlation of particles undergoing structural relaxation in previous time step. The moving particles are in red and are drawn to scale, while the particles trapped in their cages, and hence more stationary in the previous time step, are shown in blue and are drawn smaller to allow the full 3D image to be visualized. The time separation between each image is 5 minutes.
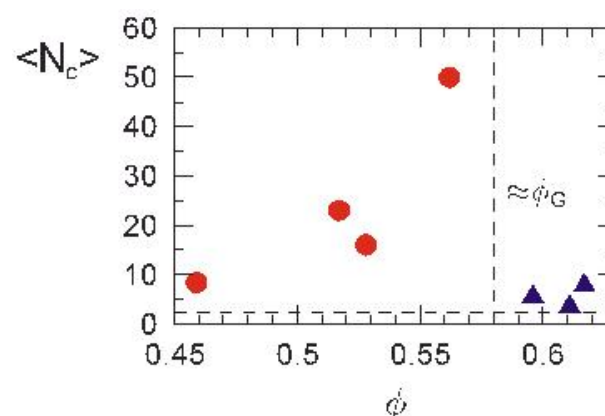

Figure 4: Average size of the correlated regions of particles undergoing structural relaxation. The size increases sharply as ϕ_g is approached, and then falls precipitously above.

When the sample is well within the glassy region, the structural relaxation occurs much more rarely, and when it does occur, it tends to be more highly localized. The characteristic time scale between relaxation events gets very long, corresponding to a large energy barrier for such a relaxation event to occur. Indeed, it is virtually impossible to observe these events in any reasonable experimental time frame.

However, they can be sped up through application of a shear strain. If this is done sufficiently slowly, local structural relaxation events are observed [FL98, SWS07].

Similar structural relaxation must also occur in granular materials, although these are more difficult to study as they are more difficult to observe in 3D. In addition, for granular materials, the dynamic heterogeneity is not thermally activated as it is in a glassy material that has not quite reached the glass transition. By contrast, similar more localized structural relaxation must occur in granular material that is flowing due to a shear stress, such as grains of sand flowing down an incline. These effects are probably best studied using colloidal particles, or these 'granular glasses.'

3   Attractive Colloidal Glasses

The interparticle interaction between the colloidal particles can be very precisely controlled. Stability of the colloidal particles against aggregation demands a very strongly repulsive interaction between the particles. For hard-sphere colloidal particles this is achieved by a very strong short range repulsion. For these repulsive particles, the phase behavior is directly determined by the volume occupied by the particles and by their crowding as ϕ increases and approaches ϕ_g. Such crowding only occurs when the volume fraction of particles fills nearly all space. However, colloidal particles are unique in that they can also have a weak attractive interaction between particles. This attraction must be sufficiently weak to ensure that the particles do not permanently stick to one another and aggregate. Instead, the attraction is typically at energy scales of only a few k_BT. However, this attractive interaction means that the system can become solid-like with a more spatially heterogeneous structure. This is commonly called gelation, but this shares many of the features of a glass transition. This behavior is actually quite common in technological uses of colloidal suspensions or other complex fluids, and thus the study of the properties of colloidal gelation is of importance both for practical purposes as well as an example of a glass transition.

This sort of colloidal glass transition, or gelation, is typically a very strongly kinetic process. The particles are destabilized and begin to aggregate; if the attraction is very large, there is no possibility for the particles to come apart once they have stuck to one another, and the aggregation is irreversible. In this case, the motion of the particles prior to sticking to one another has very important consequences for the resultant nature of the solid structure or gel. In the limit of diffusive particle motion and diffusion-limited collisions, the aggregates formed are fractal, with a fractal dimension of $d_f = 1.8$; as a result, the aggregates become more and more tenuous, and, on average, have a lower and lower density, as they grow [WO84]. Thus, the sample can form a solid gel [CG92, BMGW92] at arbitrarily low volume fractions, and the actual lower limit of ϕ that will gel is set by other factors, namely by the intrinsic strength of the gel which withstands the thermal motion, which becomes larger with larger length scales [MCT+04]. This process is known as diffusion-limited gelation. By contrast, if the attractive interaction is not as strong, there is some possibility that the bonds between particles can break, and as a result, the solid-like transition occurs at higher concentration, and the concentration that it occurs depends on the attractive energy. In this case, the particles can be very susceptible to sedimentation due to buoyancy mismatch; as a result, there are many reports in the literature of behavior which is clearly affected by gravitational collapse [PPIB94]. This tends

to obscure the underlying behavior, and thus experiments with buoyancy-matched samples are essential to fully understand the properties.

The existence of a well-defined boundary between fluid-like and solid-like states is most clearly shown by the rheological properties of the samples. The rheological behavior of weakly attractive particles exhibits a remarkable property: The data for every sample can be scaled onto a single master curve [TW00], as shown for samples of carbon black in oil at different volume fractions in Fig. 5. The interaction energy between particles can also be varied through addition of different concentrations of a dispersant, a surfactant-like molecule that adsorbs on the surface of the particles and imparts some steric stability. This results in scaling of the rheological response onto exactly the same master curve. For a fixed interaction energy and changing volume fraction, those samples with a higher ϕ have a larger elastic modulus, and their data occupy the lower frequency side of the master curve. As ϕ decreases, the elastic modulus decreases, and the data fall more and more to the higher frequency side of the master curve. The actual origin of the scaling behavior can be understood by considering a model that simply adds two contributions to the response: a frequency-independent, elastic contribution that depends on the volume fraction of particles, and viscous response that increases linearly with frequency that reflects the contribution of the background fluid to the response. Thus, the dominant response at low frequencies is the elastic response whereas at high frequencies it is the viscous response. As a result, the data must be scaled along both axes, and the relationship of the two resultant scaling parameters should be linear; this is observed. Thus, this simple model describes the behavior quite well. The important consequence of this scaling is that even when the response is too weak to clearly measure the elastic component, as occurs, for example, for samples at very low volume fractions, it is nevertheless feasible to determine the elasticity by the scaling of the data. This allows us to identify the boundary between a solid-like gel state and a fluid-like state quite precisely.

Interestingly, the behavior of the weakly attractive colloidal particles exhibits exactly the same sort of behavior as that predicted for a 'jamming' transition for granular particles [TPC+01]. Indeed, the original speculation about jamming also included a speculation that a jammed state should also exist for attractive particles; in this case, the attractive energy is what holds the system together, rather than the excluded volume of repulsive particles. Here, the control parameters are now $k_B T/U$, where U is a measure of the attractive energy of the interparticle potential, $1/\phi$ and σ, the shear stress on the sample which can cause it to fluidize. The measured jamming phase diagram for weakly attractive colloidal particles exhibits a hyperbolic shape, shown in Fig. 6, rather than the concave shape originally predicted. Indeed, more recent work on jamming now predicts a shape closer to that observed for colloidal particles.

Again, visualization of the individual colloidal particles provides important new insight into the behavior [LZC+08]. When the attractive interaction is very short range, the magnitude of the attractive interaction, as specified by $k_B T/U$, can be determined precisely by measuring the cluster mass distribution, measured for interaction energies below the gelation limit, where the clusters remain transient. These can be compared to predictions based either on analytic results obtained using a model interaction, or through simulations. Interestingly, the boundary of the solid like behavior is always found to be exactly at the boundary of spinodal decomposi-
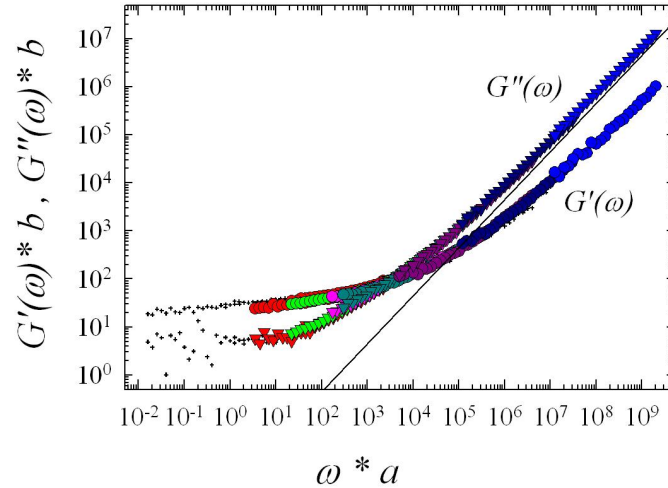
Figure 5: Scaling of the rheological response of samples of carbon black of different volume fractions. Similar behavior is observed for samples of a fixed volume fraction and varying interaction energy.
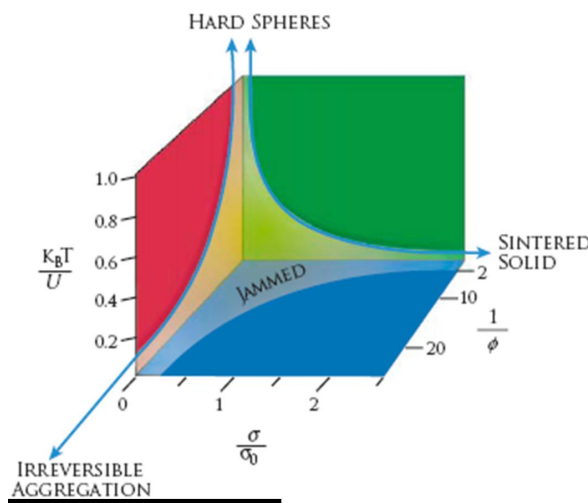

Figure 6: SJamming phase diagram for attractive colloidal particles.

tion. This suggests that the gelation, which is strictly a kinetic phenomenon, is always preceded by spinodal decomposition, which is a quasiequilibrium phenomenon. Thus, even when the system is quenched well into the gel state, the system must first pass through spinodal decomposition. This leads to phase separation into colloid-rich and colloid-poor regions, driven by spinodal decomposition. The colloid-rich region is always at high volume fractions, comparable to that of the attractive colloidal glass. As a result, the colloid-rich region undergoes a kinetic arrest, freezing in the gel state, as shown in Fig. 7. Similar behavior is observed for all attractive colloidal

systems [VAL+97]. Thus, this provides new insights into the behavior of colloidal gelation.
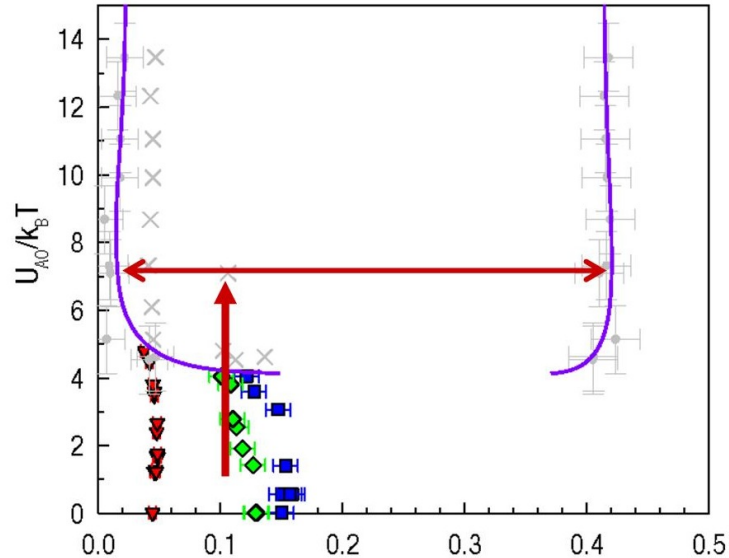

Figure 7: Model for gelation of attractive colloidal particles. A quench into the gel state initially causes spinodal decomposition into colloid-rich and colloid-poor regions. The colloid-rich region is always at the volume fraction of an attractive colloidal glass.

4   Conclusions

This paper has presented a very brief summary of results which describe the properties of colloidal particles viewed as 'granular glasses,' systems that share feature of traditional molecular glass formers and granular materials. The wealth of behavior of such granular glasses is immense, and there are many more possible analogies that have been explored by not reported here. There are even more that are awaiting further work.

References

[AGH86]   L. Antl, JW. Goodwin, and RD. Hill, *The preparation of polymethyl methacrylate latices in non-aqueous media*, Colloids Surf. **17** (1986), no. 1, 67–78.

[AMO86]   CA. Angell, DR. MacFarlane, and M. Oguni, *The Kauzmann paradox, metastable liquids, and ideal glasses*, Ann. NY Acad. Sci **484** (1986), 241–247.

[BMGW92] J. Bibette, TG. Mason, H. Gang, and DA. Weitz, *Kinetically induced ordering in gelation of emulsions*, Physical Review Letters **69** (1992), no. 6, 981–984.

[CE95]   M.T. Cicerone and MD. Ediger, *Relaxation of spatially heterogeneous dynamic domains in supercooled ortho-terphenyl*, The Journal of Chemical Physics **103** (1995), 5684.

[CG92]   M. Carpineti and M. Giglio, *Spinodal-type dynamics in fractal aggregation of colloidal clusters*, Physical Review Letters **68** (1992), no. 22, 3327–3330.

[CG96]   J.C. Crocker and D.G. Grier, *Methods of digital video microscopy for colloidal studies*, Journal of Colloid and Interface Science **179** (1996), no. 1, 298–310.

[DGP99]   C. Donati, S.C. Glotzer, and P.H. Poole, *Growing spatial correlations of particle displacements in a simulated liquid on cooling toward the glass transition*, Physical Review Letters **82** (1999), no. 25, 5064–5067.

[FL98]   ML. Falk and JS. Langer, *Dynamics of viscoplastic deformation in amorphous solids*, Physical Review E **57** (1998), no. 6, 7192–7205.

[JNB96a]   H.M. Jaeger, S.R. Nagel, and R.P. Behringer, *Granular solids, liquids, and gases*, Reviews of Modern Physics **68** (1996), no. 4, 1259–1273.

[JNB96b]   _____, *The physics of granular materials*, Physics Today **49** (1996), no. 4, 32–39.

[LN98]   A.J. Liu and S.R. Nagel, *Jamming is not just cool any more*, Nature **396** (1998), no. 6706, 21–22.

[LZC⁺08]   P.J. Lu, E. Zaccarelli, F. Ciulla, A.B. Schofield, F. Sciortino, and D.A. Weitz, *Gelation of particles with short-range attraction*, Nature **453** (2008), no. 7194, 499–503.

[MCT⁺04]   S. Manley, L. Cipelletti, V. Trappe, AE. Bailey, RJ. Christianson, U. Gasser, V. Prasad, PN. Segre, MP. Doherty, S. Sankaran, et al., *Limits to gelation in colloidal aggregation*, Physical Review Letters **93** (2004), no. 10, 108302.

[MD97]   N. Menon and D.J. Durian, *Particle motions in a gas-fluidized bed of sand*, Physical Review Letters **79** (1997), no. 18, 3407–3410.

[MW95]   TG. Mason and DA. Weitz, *Linear viscoelasticity of colloidal hard sphere suspensions near the glass transition*, Physical Review Letters **75** (1995), no. 14, 2770–2773.

[PPIB94]   PN. Pusey, WCK. Poon, SM. Ilett, and P. Bartlett, *Phase behaviour and structure of colloidal suspensions*, Journal of Physics Condensed Matter **6** (1994), 29–29.

[PVM86]   PN. Pusey and W. Van Megen, *Phase behavior of concentrated suspensions of nearly hard colloidal spheres*, Nature **320** (1986), no. 6060, 340–342.

[PVM87]   _____, *Observation of a glass transition in suspensions of spherical colloidal particles*, Physical Review Letters **59** (1987), no. 18, 2083–2086.

[SRS91]   K. Schmidt-Rohr and HW. Spiess, *Nature of nonexponential loss of correlation above the glass transition investigated by multidimensional NMR*, Physical Review Letters **66** (1991), no. 23, 3020–3023.

[SWS07]   P. Schall, D.A. Weitz, and F. Spaepen, *Structural rearrangements that govern flow in colloidal glasses*, Science **318** (2007), no. 5858, 1895.

[TPC⁺01]   V. Trappe, V. Prasad, L. Cipelletti, PN. Segre, and DA. Weitz, *Jamming phase diagram for attractive particles*, Nature **411** (2001), no. 6839, 772–775.

[TW00]   V. Trappe and DA. Weitz, *Scaling of the viscoelasticity of weakly attractive particles*, Physical Review Letters **85** (2000), no. 2, 449–452.

[VAL⁺97]   N.A.M. Verhaegh, D. Asnaghi, H.N.W. Lekkerkerker, M. Giglio, and L. Cipelletti, *Transient gelation by spinodal decomposition in colloid-polymer mixtures*, Physica A **242** (1997), 104–118.

[VBW95]   A. Van Blaaderen and P. Wiltzius, *Real-space structure of colloidal hard-sphere glasses*, Science **270** (1995), 1177–1177.

[VMU93]   W. Van Megen and SM. Underwood, *Glass transition in colloidal hard spheres: Mode-coupling theory analysis*, Physical Review Letters **70** (1993), no. 18, 2766–2769.

[WCL⁺00]   E.R. Weeks, JC. Crocker, A.C. Levitt, A. Schofield, and DA. Weitz, *Three-dimensional direct imaging of structural relaxation near the colloidal glass transition*, Science **287** (2000), no. 5453, 627.

[WO84]   DA. Weitz and M. Oliveria, *Fractal structures formed by kinetic aggregation of aqueous gold colloids*, Physical Review Letters **52** (1984), no. 16, 1433–1436.

[WW02]   E.R. Weeks and DA. Weitz, *Properties of cage rearrangements observed near the colloidal glass transition*, Physical Review Letters **89** (2002), no. 9, 95704.